Pergamon

Comput. Biol. Med. Vol. 26, No. 2, pp. 97–111, 1996

Printed in Great Britain
0010-4825/96 $15.00 + 0.00

0010-4825(95)00046-1

A NEURO-FUZZY ALGORITHM FOR DIAGNOSIS OF CORONARY ARTERY STENOSIS

LES M. SZTANDERA,* LUCY S. GOODENDAY† and KRZYSZTOF J. CIOS‡

* Department of Computer Science, Philadelphia College of Textiles and Science, Philadelphia, PA 19144, U.S.A.; † Department of Nuclear Cardiology, Medical College of Ohio, Toledo, OH 43699, U.S.A.; and ‡ Department of Electrical Engineering, University of Toledo, Toledo, OH 43606, U.S.A.

(*Received* 29 *July* 1993; *received in revised form* 23 *August* 1995)

Abstract—In this paper a method of fuzzy decision making applied to diagnosis of coronary artery stenosis is presented. The method uses a neural network approach for the diagnosis of stenosis in the three main coronary arteries (left anterior descending, right coronary artery, and circumflex). First, the knowledge base domain, 201Tl scintigram training data, is explained and the method of preprocessing the original heart images is given. Next, the method of dealing with the uncertainties present in the data using the fuzzy approach is outlined. Finally, the algorithm and the results are discussed and compared with other approaches.

Fuzzy decision making Neural networks Medical diagnosis Thallium-201 imaging

1. INTRODUCTION

Diagnosing obstructions in the three main coronary arteries from myocardial perfusion scintigrams has been a major area for research over the years. Stenosis in the main arteries supplying the myocardium is the most common underlying cause of heart attacks. Determination of how severely a coronary artery blockage interferes with blood flow to the myocardium, and which arteries are stenosed, is important in determining the best type of treatment for the particular patient. Methods of gathering information about the patency or stenosis of the main coronary arteries, i.e. left anterior descending (LAD), right coronary artery (RCA), and left circumflex artery (CCX), without performing an invasive procedure are important to the practice of cardiology. The most direct way to learn the site of coronary stenosis is by performing coronary arteriography. This is an invasive procedure which involves the introduction of radiodense material into the coronary arteries via an intravascular catheter. This procedure entails risk and discomfort to the patient. Moreover, the procedure gives little information regarding the functional significance of the stenoses.

A procedure that is less invasive, the stress 201Tl scintigraphy, has been used in nuclear cardiology to detect abnormalities [1] in the distribution of the blood flow to the myocardium. Scintigrams have been used to determine which regions of the heart have a less than normal amount of blood flow, thus having perfusion defects. By comparing the scintigram of a patient to pooled scintigraphic data obtained from normal subjects it can be shown [2] that there is a relationship between different regions of the heart where perfusion defects are located and the location of the coronary stenosis. Since physicians vary in skill, experience and consistency of interpretation, a neural network algorithm was proposed to improve the consistency of diagnosis. To represent uncertainties associated with the diagnostic concepts, fuzzy decision making was chosen.

2. DATA COLLECTION AND PROBLEM STATEMENT

Stress Tl-201 scintigraphs were obtained from patients with arteriographically proven single-vessel coronary artery obstructions, and from patients with arteriographically

proven normal coronary arteries and normal ventricular function. Tl-201 scintigrams were collected after maximal exercise from the 78 kV photopeak with a 20% window, using a portable gamma camera equipped with a 1/4 inch crystal and high-resolution collimator. Three views of the left ventricle—anterior (ANT), left lateral (LAT) and left anterior oblique (LAO)—required approximately 10 min each with minimum of 300,000 scintillation counts collected in each view [2]. The goal of the stress is to direct a greater portion of the blood supply to the myocardial region, so as to obtain a greater contrast between those regions of the heart that are ischemic (having a local lack of blood supply) and those regions that are normal. The ischemic areas are known as perfusion defects. The major cause of such perfusion defects is known to be stenosis of the coronary arteries defined by us as reduction of cross-sectional area of an artery's lumen by at least 70%. In order to partially overcome the problem of the wide variations in the anatomy of a heart, yet still be able to make meaningful relative comparisons of different hearts, a normalized planar view of the heart from each of the three different camera angles: anterior, left lateral and left anterior oblique was proposed [1]. The views were not compensated for washout of the 201Tl caused by the redistribution and decay of the 201Tl over time, because it is assumed that if differences exist in each of the three views due to the washout, these differences would be small in relative magnitude and would not substantially affect the resultant distribution of the defect image. With this assumption, each of the views was normalized by the method described below, and was later subjected to intraview and interview comparisons. The perimeter of the scintigraphic image of the left ventricle of the heart was scanned and traced by the operator. Then the apex and the right aortic root points were identified to the computer procedure through the direction of the operator. The computer procedure then generated an axis that extends from the center of the base to the apex of the heart. This axis provided the basis from which the remainder of the grid system of the normalized heart space was constructed. Forty equally spaced horizontal axes were instated orthogonal to the apex/base axis. Each of these axes was subdivided into 100 equal regions, where the limit of the subdivision for each horizontal axis was the intersection of the horizontal axis with the perimeter of the left ventricle. This scheme is depicted in Fig. 1. Count densities from each of the 4000 regions (40×100 grid) have a minimum of 750 counts cm^{-2} after correction for background level. The correction for background level consists of subtracting the count density of the area of the chest wall from each region. After a nine point smoothing technique has been applied to reduce the noise, the image in its intermediate state is visually scanned by the operator to find the area of highest count density. A sample area (area "A") of the highest count density is shown in Fig. 1. The operator designates various trial areas which are tested to determine the highest count density, under the constraint that at least 20 pixels be included in the area accepted by the operator as the area of maximum count activity density. The entire image is then divided by this maximum count activity density to yield normalized count activity ratios,

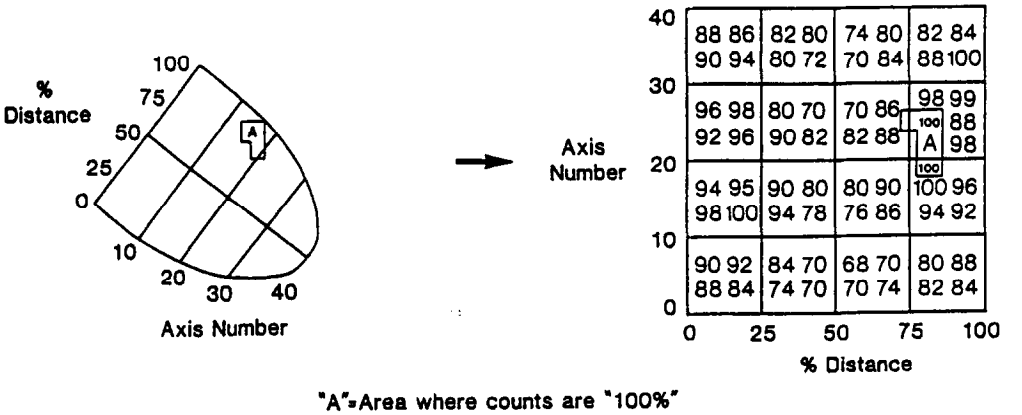

Fig. 1. Axis system of normalized left ventricular image representation.

Table 1. Formation of 10 consolidated regions from perfusion defect image

Region	Horizontal axes included (apex = 40)	Vertical axes included (right = 100)
1	1–13	1–25
2	1–13	26–50
3	1–13	51–75
4	1–13	76–100
5	13–26	1–25
6	13–26	26–50
7	13–26	51–75
8	13–26	76–100
9	26–40	1–50
10	26–40	51–100

expressed in terms of percentage of the maximum count activity. The idea is depicted in Fig. 1. For the heart images of normal patients, first and second order statistics of the normalized count activity ratios are calculated for each of the 4000 regions, and used to establish a "normal template". The scintigrams are then processed by comparing the normalized count ratio for each pixel at a given anatomic location with that obtained from the normal template. Pixels containing count ratios that fell more than 2.5 standard deviations below normal are considered to be underperfused. Then a defect is recorded and displayed on the image with the intensity of the pixel being directly proportional to the numerical distance of the normalized count activity ratio from the normal template mean. If the count activity ratio was in excess, and is consequently not rejected by the one tailed mean test, then the pixel is turned off. The 4000 regions were brought together into 10 regions that consolidated on the basis of axis in the 40×100 grid system. The consolidation was accomplished in accordance with specifications listed in Table 1. Thus each of the three views was divided into 10 anatomic regions called segments. However, for computer analysis, the regions of all three views were numbered consecutively. Segments 1–10 of the anterior view are referred to as regions 1–10, segments 1–10 of the left lateral view are referred to as regions 11–20, and segments 1–10 of the left anterior oblique view are referred to as regions 21–30. The percentage of underperfused (as compared with normally perfused) pixels in each region represents the magnitude of the perfusion defect for that region. Thus, 30 numbers ranging in size from 0 to 100, each representing the size of the perfusion defect in that region, were generated from each patient scintigram. Figure 2 shows the numbering scheme. Those thirty-dimensional vectors collected from 91 patients, who underwent thallium-201 myocardial scintigraphy, were used as inputs for the neuro-fuzzy algorithm [3]. The use of fuzzy decision making is necessitated in order to capture the uncertainties in a digital image. Numerous previous attempts were utilized to attack the problem, however the results were not satisfactory. The fuzzy set theory approach seems to be appropriate in tackling the problem, as it provides a suitable means for analyzing complex systems and decision making processes when the pattern indeterminacy is caused by the inherent variability and fuzziness rather than randomness. Thus, the fuzzy methodology is utilized to increase the amount of information available in decision making. In the proposed approach the fuzzy membership functions are learned by a neural network from the data. In our case, 64 scans were chosen at random for training and the remaining 27 scans were used for testing. The major coronary arteries are classified as the left anterior descending artery (LAD), right coronary artery (RCA), circumflex artery (CCX), and the posterior descending artery. For the data analysis, however, patients having a significant stenosis upstream from the posterior descending artery were classified as having right coronary artery obstruction, regardless of whether this artery arises from the right coronary or circumflex artery. Thus, the training file consists of 64 thirty-dimensional vectors which are assigned to the following classes: eight vectors representing patients with CCX, 22 with LAD, 16 with RCA and 18 normal patients. The testing file consists of 27 thirty-dimensional vectors.

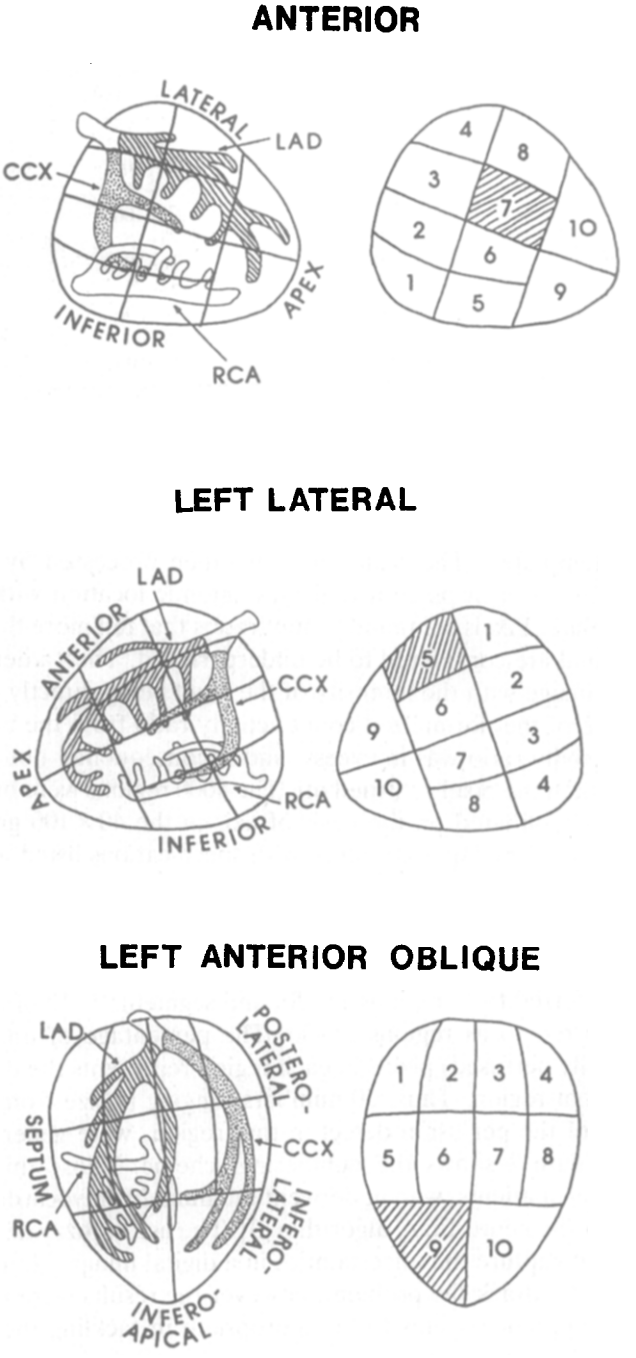

Fig. 2. Three views of a scan and the numbering scheme for the segments of each view: CCX stands for circumflex artery, LAD for left anterior descending artery, and RCA for right coronary artery.

Three of them representing CCX, 10 representing LAD, seven representing RCA and seven representing data collected from normal patients. These data sets were used by the neural network algorithm and in fuzzy decision making. The techniques are outlined in the next section.

3. A HYBRID NEURO-FUZZY ALGORITHM

The proposed algorithm generates a feed forward network architecture for the Tl-201 scintigraph problem, and after having generated fuzzy subsets at each node of the network, it switches to fuzzy decision making on those subsets. The nodes and hidden

layers are added until a learning task is accomplished. The algorithm operates on continuous data and equates a decision tree with a hidden layer of a neural network [3]. A learning strategy used in this approach is based on minimization of the entropy function. This minimization of entropy translates into adding new nodes to the network until the entropy is reduced to zero. When the entropy is zero then all training examples are regarded as correctly recognized. The incorporation of fuzzy sets into the algorithm seems to result in a drastic reduction of the number of nodes in the network, and in decrease of the convergence time. Connections between the nodes have a "cost" function being equal to the weights of a neural network. The directional vector of a hyperplane, which divides decision regions, is taken as the weight vector of a node.

Let us repeat here the basic notation after [3]. There are N training examples, N^+ examples belonging to class "+", and N^- examples belonging to class "−". A hyperplane divides the examples into two groups: those lying on the positive (1) and negative (0) sides of it. Thus, we have four possible outcomes:

$$\begin{aligned} &N_1^+ \text{—number of examples from class "+" on the side 1,}\\ &N_0^+ \text{—number of examples from class "+" on the side 0,}\\ &N_1^- \text{—number of examples from class "−" on the side 1,}\\ &N_0^- \text{—number of examples from class "−" on the side 0.} \end{aligned} \tag{1}$$

Let us assume that at a certain level of a decision tree N_r examples are divided by a node r into N_r^+ belonging to class "+", and N_r^- belonging to class "−". The values N_{1r}^+ and N_{1r}^- are calculated as follows:

$$N_{1r}^+ = \sum_{i=1}^{N} D_i \,\mathrm{out}_i \tag{2}$$

$$N_{1r}^- = \sum_{i=1}^{N_r} (1 - D_i)\,\mathrm{out}_i, \tag{3}$$

where D_i stands for the desired output, and out_i is a sigmoid function.
Thus, we have:

$$\begin{aligned} N_{1r}^+ + N_{1r}^- &= \mathrm{out}_1 + \cdots + \mathrm{out}_{N_r}\\ &= \sum_{i}^{N_r} \mathrm{out}_i = \sum_{i}^{N_r} \left[1 + \exp\left(\sum_j w_{ij} x_j\right)\right]^{-1} \end{aligned} \tag{4}$$

The change in the number of examples, on both positive and negative sides of a hyperplane, with respect to weights is given by [3]:

$$\Delta N_{1r}^+ = \sum_{i=1}^{N_r} D_i \,\mathrm{out}_i(1 - \mathrm{out}_i) \sum_j x_j \Delta w_{ij} \tag{5}$$

$$\Delta N_{1r}^- = \sum_{i=1}^{N_r} (1 - D_i)\,\mathrm{out}_i(1 - \mathrm{out}_i) \sum_j x_j \Delta w_{ij}. \tag{6}$$

The learning rule to minimize the fuzzy entropy $f(F)$ [3] is:

$$\Delta w_{ij} = -\rho \frac{\partial f(F)}{\partial w_{ij}} \tag{7}$$

where ρ is a learning rate, and $f(F)$ is a fuzzy entropy function.

The grades of membership for fuzzy sets F and F^C to be used in calculation of $f(F)$ are defined as follows:

$$F = \left\{ \frac{N_{0r}^-}{N_{0r}}, \frac{N_{0r}^+}{N_{0r}}, \frac{N_{1r}^-}{N_{1r}}, \frac{N_{1r}^+}{N_{1r}} \right\} \tag{8}$$

$$F^C = 1 - F. \tag{9}$$

If we use the mutual dependence of positive and negative examples on both sides of a hyperplane, then, taking into account that $N_{1r} = N_{1r}^{+} + N_{1r}^{-}$ and $N_{0r} = N_{0r}^{+} + N_{0r}^{-}$, the resulting fuzzy set F and its complement F^C are defined as:

$$F = \left\{ \frac{N_r^- - N_{1r}^-}{N_r - N_{1r}^+ - N_{1r}^-}, \frac{N_r^+ - N_{1r}^+}{N_r - N_{1r}^+ - N_{1r}^-}, \frac{N_{1r}^-}{N_{1r}}, \frac{N_{1r}^+}{N_{1r}} \right\} \tag{10}$$

$$F^C = \left\{ \frac{N_r^+ - N_{1r}^+}{N_r - N_{1r}^+ - N_{1r}^-}, \frac{N_r - N_{1r}^- - N_r^+}{N_r - N_{1r}^+ - N_{1r}^-}, \frac{N_{1r} - N_{1r}^-}{N_{1r}}, \frac{N_{1r} - N_{1r}^+}{N_{1r}} \right\}. \tag{11}$$

The four grades of membership (equations (10) and (11)) are used in Dombi's operations [4] specified by equations (12) and (13) below (with $F^C = H$):
Fuzzy union

$$\mu_{FUH}(x) = \frac{1}{1 + \left[\left(\frac{1}{\mu_F(x)} - 1 \right)^{-\lambda} + \left(\frac{1}{\mu_H(x)} - 1 \right)^{-\lambda} \right]^{-1/\lambda}} \tag{12}$$

Fuzzy intersection

$$\mu_{F \cap H}(x) = \frac{1}{1 + \left[\left(\frac{1}{\mu_F(x)} - 1 \right)^{\lambda} + \left(\frac{1}{\mu_H(x)} - 1 \right)^{\lambda} \right]^{1/\lambda}} \tag{13}$$

where λ is a parameter by which different unions/intersections are distinguished, $\lambda \varepsilon (0, \infty)$. It is also assumed here, after [4], that Dombi's union equals one if the grades of membership $\mu_F(x)$ and $\mu_H(x)$ are both one, and Dombi's intersection equals zero if they are both zero. The parameter λ has to be estimated for a particular application. Then the fuzzy entropy measure is calculated according to the formula

$$f(F) = \frac{\sum \text{count}(F \cap F^C)}{\sum \text{count}(F \cup F^C)}, \tag{14}$$

where Σ count (sigma-count) is the cardinality of a fuzzy set.

Obtained fuzzy entropy is used to calculate the weights using learning rule (7). In order to increase the chance of finding the global minimum the learning rule is also combined with Cauchy training [5] in the same manner as suggested in [3]:

$$W_{k+1} = W_k(1 - \zeta)\Delta W + \zeta \Delta W_{\text{random}}, \tag{15}$$

where ζ is a control parameter.

The algorithm generates fuzzy subsets A and B at each node. The grades of membership for the fuzzy subsets A and B are initially defined for only two points "m_1" and "m_2" from which we construct the two fuzzy subsets. The points "m_1" and "m_2" are chosen experimentally.

The grades of membership for fuzzy sets A and B, at points "m_1" and "m_2" are depicted in Fig. 3, and are defined as follows:

$$\mu_A(m_1) = \frac{N_{0r}^-}{N_{0r}}, \mu_A(m_2) = \frac{N_{0r}^+}{N_{0r}}$$

and

$$\mu_B(m_1) = \frac{N_{1r}^-}{N_{1r}}, \mu_B(m_2) = \frac{N_{1r}^+}{N_{1r}}. \tag{16}$$

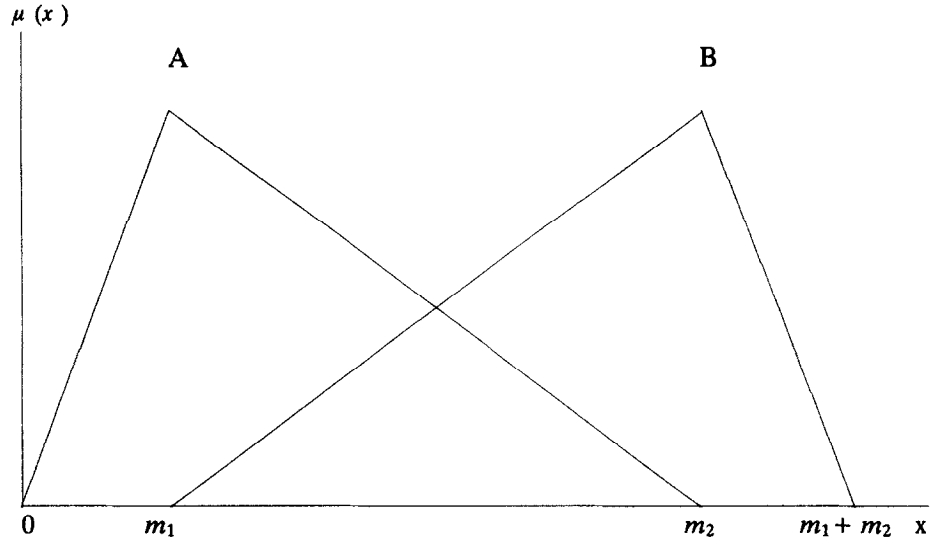

Fig. 3. Sample fuzzy subsets generated at one of the nodes.

Taking into account that $N_{1r} = N_{1r}^{+} + N_{1r}^{-}$ and $N_{0r} = N_{0r}^{+} + N_{0r}^{-}$ results in the following expressions:

$$\mu_A(m_1) = \frac{N_{0r}^{-}}{N_{0r}^{+} + N_{0r}^{-}} = \frac{N_r^{+} - N_{1r}^{+}}{N_r - N_{1r}^{+} - N_{1r}^{-}},$$

$$\mu_A(m_2) = \frac{N_{0r}^{+}}{N_{0r}^{+} + N_{0r}^{-}} = \frac{N_r^{-} - N_{1r}^{-}}{N_r - N_{1r}^{+} - N_{1r}^{-}}$$

$$\mu_B(m_1) = \frac{N_{1r}^{-}}{N_{1r}^{+} + N_{1r}^{-}}, \mu_B(m_2) = \frac{N_{1r}^{+}}{N_{1r}^{+} + N_{1r}^{-}}. \tag{17}$$

Now, we define membership grades for the fuzzy sets A and B from the following functions:

$$\mu_A(x) = \begin{cases} \dfrac{x\mu_A(m_1)}{m_1} & \text{for } x \leq m_1 \\ \dfrac{\mu_A(m_2)(x - m_1) + \mu_A(m_1)(m_2 - x)}{m_2 - m_1} & \text{for } m_1 \leq x \leq m_2 \\ 0 & \text{for } x > m_2 \end{cases}$$

$$\mu_B(x) = \begin{cases} 0 & \text{for } x < m_1 \\ \dfrac{\mu_B(m_2)(x - m_1) + \mu_B(m_1)(m_2 - x)}{m_2 - m_1} & \text{for } m_1 \leq x \leq m_2 \\ \dfrac{\mu_B(m_2)((m_1 + m_2) - x)}{m_1} & \text{for } m_2 \leq x \leq m_1 + m_2 \\ 0 & \text{for } x > m_1 + m_2. \end{cases} \tag{18}$$

If at a certain level we have more than one subset A, and more than one subset B then we perform max operation to get the resulting grades of membership for just one A and one B. These sets are then used in the fuzzy decision making process—ranking of fuzzy sets.

The algorithm uses the fuzzy decision making criteria.

Fuzzy decision making criteria

For fuzzy subsets A and B, specified at some node of a network, the classification is based on the following definition (Definition 1) [3].

Definition 1. The ranking of fuzzy subsets is faithful, i.e. the data samples are fully

separated if the following values for the ranking indices are established:

$$x_A = \frac{1}{3}(m_1 + m_2), x_B = \frac{2}{3}(m_1 + m_2) \tag{19}$$

using either Yager's F1 [6] index or the centroidal method [7]. These indices (19) correspond to fuzzy entropy equaling zero. More information about the above ranking indices is given in [8].

Multicategory classifier

We will now consider recognition of C classes, where $C > 2$. The concepts introduced before will be used; however, the final nodes of the tree corresponding to the neural network will be associated now with two of the C classes (instead of one of two classes). We propose a new strategy based on adequate dichotomization of the classes.

Our approach is to use the algorithm which now runs $(C-1)$ ranking subroutines, each trying to achieve ranking indices specified by Definition 1, thus separating patterns of class c from all other patterns, and then repeating the procedure until c equals $C-1$. The fuzzy sets are formed and ranked for class c (the first fuzzy set) and for all $(c-1)$ classes combined together (the second fuzzy set).

The outline of the whole approach follows. The algorithm has five steps. Step 1 divides the input space into several subspaces; Step 2 counts the number of samples in those subspaces; Step 3 generates membership functions of fuzzy subsets out of those numbers; Step 4 executes ranking of formed fuzzy subsets; Step 5 determines separation of categories based on faithful ranking.

Step 1—Divide the input space into several subspaces

First, we make use of the learning rule (7) and search for a hyperplane that minimizes the entropy function:

$$\min_{W_i} f(F) = \sum_{r=1}^{R} \frac{N_r}{N} \text{entropy}(L, r),$$

where L is a level of a decision tree, R is the total number of nodes in a layer, r is the number of nodes, $f(F)$ is the entropy function.

Step 2—Count the number of samples in resulting subspaces

Use here the notation specified in (1). The first class consists of patterns belonging to class c, and the other class consists of all other patterns. Start with random initial vector W_0.

Step 3—Generate membership functions for fuzzy subsets

Generate membership functions, using Definition 1, for fuzzy subsets while creating nodes in hidden layers.

Step 4—Execute ranking of the formed fuzzy subsets

The ranking is executed according to the Yager F1 index [7] with $g(u) = u$ or Murakami *et al.* [8] centroidal method for x_0.

$$F1(A_i) = \frac{\int_0^1 g(u)\mu_{A_i}(u)\,du}{\int_0^1 \mu_{A_i}(u)\,du},$$

or

$$x_0 = \frac{\int_0^1 u\mu_{A_i}(u)\,du}{\int_0^1 \mu_{A_i}(u)\,du} \tag{20}$$

Step 5—Determine separation of categories based on faithful ranking

The ranking of fuzzy subsets is faithful, i.e. the data samples are fully separated if the values for the ranking indices (19) are established.

If this is the case then increase c by 1 and return to step 1. Continue until $c = C - 1$. If the ranking is unfaithful, add a new node into the current layer and go to Step 1.

To justify the validity of the approach, the method has been applied to various benchmark problems, and the outcomes were favorable as compared to other types of neural networks (e.g. backpropagation and quickpropagation) [3]. However, as the proof of any new technology ultimately lies in its utility for solving real life problems, the technique was verified on the Tl-201 scintigraph data.

4. RESULTS

Using the proposed algorithm, and 75% of the data for training, the feedforward neural network architecture depicted in Fig. 4 was generated. The training file consisted of 64 thirty-dimensional vectors which were assigned to the following classes: eight vectors representing patients with CCX, 22 with LAD, 16 with RCA, and 18 normal patients. The remaining 25% of the available data vectors, 3 of them representing CCX, 10 representing LAD, 7 representing RCA, and 7 representing data collected from normal patients, were used for testing.

Using the neural network to define grades of membership for fuzzy sets, and then ranking of these sets in a fuzzy decision making process, all the patients from the 25% testing pool have been classified correctly. The advantage of the proposed algorithm can

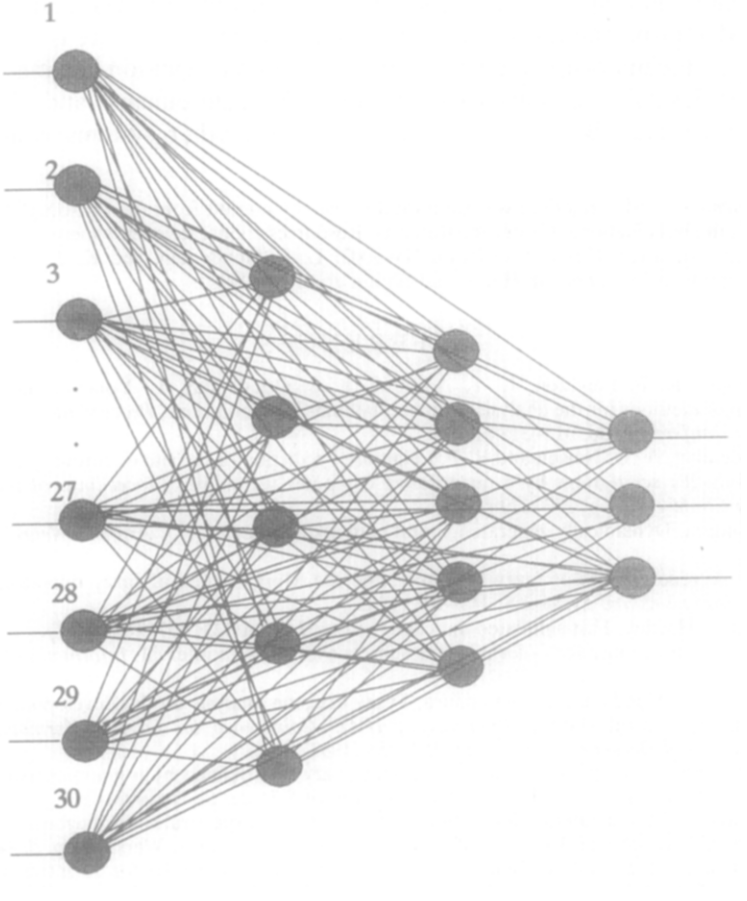

Fig. 4. A neural network architecture for the Tl-201 scintigram problem.

Table 2. Summary of the results, in percentage of proper classification, for the proposed neuro-fuzzy algorithm and other approaches

Location/of stenosis/ Method used	RCA artery	CCX artery	LAD artery	Normal
Neuro-fuzzy algorithm	100%	100%	100%	100%
Rule aggregation EXP	89%	93%	85%	96%
Rule aggregation CLILP2	89%	52%	63%	100%
Rule aggregation ALFS	89%	89%	85%	100%

be seen by comparison with previously obtained results which utilized other approaches [9, 10]. The superiority of the hybrid neuro-fuzzy approach lies in its ability of accessing and manipulating high dimensional arrays (in this particular case thirty-dimensional). In all other approaches some important information was lost while using dimensionality reduction techniques. The results are summarized in Table 2.

5. CONCLUSIONS

The concept of utilizing fuzzy set theory with neural networks seems to be an extremely powerful and promising technology. Our results for detecting obstructions in coronary arteries verify that claim.

The main features and advantages of the proposed algorithm are: (1) it is a simple and straightforward quick-pass build-up procedure, where no time-consuming iterative training is required, resulting in much shorter design time than most of neural networks; (2) it is a general method of how to use numerical information, via neural networks, to provide good approximations to the membership functions; (3) there is a lot of freedom in choosing the membership functions of fuzzy sets used in decision making; this provides flexibility for designing systems satisfying different requirements; and (4) it performs successfully on data, like Tl201 scintigraphs, where other systems would not work perfectly.

Acknowledgements—L. M. Sztandera was supported in part by a grant from the Pittsburgh Supercomputing Center through the NIH National Center for Research Resources cooperative agreement 1 P41 RR06009, and by a grant from American Heart Association NW9002. L. S. Goodenday and K. J. Cios would like to acknowledge support from American Heart Association grant NW9002.

REFERENCES

1. A. D. Nelson, R. F. Leighton, L. T. Andrews, L. S. Goodenday, L. Yonovitz and D. Thekdi, A comparison of methods for the analysis of stress thallium-201 scintigrams, *Proceedings of the Computers in Cardiology Conference*, pp. 315–318 (1979).
2. L. S. Goodenday, A. D. Nelson and R. F. Leighton, Prediction of the site of coronary artery obstruction from thallium-201 scintigrams by a quantitative computer technique, *Proceedings of the Computers in Cardiology Conference*, pp. 277–279 (1981).
3. L. M. Sztandera, Dynamically generated neural network architectures, *J. Artificial Neural Systems*, **1**, 41–66 (1994).
4. J. Dombi, A general class of fuzzy operators, the De Morgan class of fuzzy operators and fuzziness measures, *Fuzzy Sets and Systems* **8**, 149–163 (1982).
5. H. Szu and R. Hartley, Fast simulated annealing, *Phys. Lett. A* **122**, 157–162 (1987).
6. R. R. Yager, A procedure for ordering fuzzy subsets over the unit interval, *Information Sci.* **24**, 143–161 (1981).
7. S. Murakami, H. Maeda and S. Immamura, Fuzzy decision analysis on the development of centralized regional energy control system, *Preprints of IFAC Conference on Fuzzy Information, Knowledge Representation and Decision Analysis*, pp. 353–358 (1983).
8. L. M. Sztandera, A comparative study of ranking fuzzy sets defined by a neural network algorithm—justification for a centroidal method, *Archives of Control Sciences* 5–25 (1995).
9. K. J. Cios and L. M. Sztandera, Generation of fuzzy sets and expert rules for diagnosis of heart disease, *Proceedings of International AMSE Conference on Signals and Systems*, Warsaw, pp. 37–44 (1991).
10. K. J. Cios and L. M. Sztandera, Generation of fuzzy sets and expert rules for diagnosis of heart disease, *Proceedings of the 4th International Symposium on Fuzzy Systems and Signals*, Warsaw, pp. 101–108 (1991).

About the Author—LES M. SZTANDERA (PhD, University of Toledo, M.S., University of Missouri-Columbia, Diploma, Cambridge University) is Assistant Professor of Computer Science at Philadelphia College of Textiles and Science, Philadelphia, PA 19144. His research interests include fuzzy logic, neural networks, pattern recognition, computer vision, and modeling and management of uncertainty. Dr Sztandera is a member of the North American Fuzzy Information Processing Society (NAFIPS), and Canadian Society for Fuzzy Information and Neural Systems.

About the Author—LUCY S. GOODENDAY (M.D., New York Medical College, B.A., Bryn Mawr College) is Associate Professor of Medicine in the Cardiology Division, and Director of Nuclear Cardiology at the Medical College of Ohio, Toledo, OH 43699. Dr Goodenday has practiced and carried out research in nuclear cardiology for 16 years now. Her special interests include application of computer techniques to medical diagnosis.

About the Author—KRZYSZTOF J. CIOS (M.B.A., University of Toledo, M.S., PhD, Academy of Mining and Metallurgy, Poland) is Associate Professor of Electrical Engineering at the University of Toledo, Toledo, OH 43606. His research interests are in neural networks, machine learning, fuzzy and knowledge based systems. He is a senior member of IEEE and the Computer Society. He is also a member of the Sigma Xi Scientific Research Society.

APPENDIX
CONNECTION WEIGHTS OBTAINED FOR THE TI-201 SCINTIGRAM PROBLEM

2 30		
0.007145	0.010446	0.071787
-0.023418	0.030893	-0.011383
0.003527	0.007073	0.012670
-0.009059	0.004053	0.019841
-0.000191	-0.004516	-0.007187
0.014846	-0.005912	-0.012894
0.005240	0.028492	0.002010
0.016149	-0.001367	0.015055
0.009080	0.014376	-0.007434
-0.010437	0.031951	0.004540
-0.091745	0.979777	0.421300
0.552862	0.161894	-3.776138
-0.061577	-1.210332	0.621754
0.570373	-0.527696	-0.466523
-0.352787	-0.482462	1.238135
-0.967417	-1.000351	-0.071902
-0.236777	0.136607	0.098434
0.186523	-0.033685	-0.032432
-0.209937	4.954815	0.204379
0.744294	0.273584	0.671317

2 32		
0.007703	-0.008776	0.024500
0.007628	-0.014201	0.001805
0.004088	-0.007929	-0.016710
0.006112	0.004940	0.001955
-0.003476	0.010508	-0.004419
-0.016015	0.004593	0.003564
-0.004382	-0.014611	-0.011027
-0.024385	0.004294	0.005242
0.000243	-0.025132	-0.000912
0.001473	-0.017957	-0.008921
-0.531954	0.069003	
-0.366917	0.118144	-0.127219
-0.243529	-0.347431	0.193454
4.999999	0.154156	-0.076126

APPENDIX Continued

-0.170833	0.283881	0.093271
0.139639	0.128347	-0.126437
-0.153700	0.080018	-0.046215
0.032371	-0.873635	-0.055733
0.050099	-0.009233	-0.068125
-2.094025	1.054276	0.093697
0.054319	-0.387830	0.354515
0.005516	0.110636	

1 34		
0.026585	0.010168	-0.005216
0.001458	0.002103	-0.004942
-0.002212	-0.005248	0.001504
0.011514	0.004789	0.000456
-0.004274	-0.001591	0.025408
0.001151	0.038688	0.001054
0.011727	-0.002525	-0.013559
-0.008797	-0.005356	-0.003707
0.002203	0.005551	0.001568
-0.000599	-0.000030	-0.003177
-0.018701	0.011023	-0.000952
-0.003617	0.000352	-0.159313
0.006226	-0.007188	0.001898
-0.004200	0.002542	-0.004047
0.048688	0.012037	-0.748673
-0.004765	0.012498	-0.012925
-0.025546	-0.495951	-0.072943
0.002040	0.001834	0.019367
0.007906	0.101880	0.035063
-0.009301	0.007306	0.002880

3 30		
0.010862	0.014430	-0.008001
-0.002699	-0.004773	0.002017
0.021058	-0.009838	-0.002697
0.010302	-0.010006	0.007837
-0.027434	-0.057154	0.020767
0.002445	0.017274	-0.028897
0.001716	0.002739	-0.016767
0.008626	0.013645	-0.003084

APPENDIX Continued

0.016894	0.001790	0.005958
-0.036389	0.003911	-0.009150
-0.008696	-0.010207	0.024652
-0.005173	-0.009137	-0.006132
0.015103	-0.018419	0.009033
-0.000631	-0.011125	-0.001749
0.000268	0.003643	-0.008714
-0.080434	-0.004649	0.004274
0.012275	0.011587	0.007453
-0.004392	0.006445	0.035358
-0.000053	0.006705	0.005921
-0.007321	-0.003769	0.010491
0.107854	-0.007031	0.166889
-0.102072	0.024710	0.021152
0.132417	-0.065565	-0.025533
0.048834	-0.051726	0.120234
0.044534	0.008085	0.130942
0.065391	-0.257412	-0.120295
0.079216	-0.015063	0.073995
0.021991	0.051388	-0.229866
0.010808	-0.034508	-0.059572
0.051790	-0.224385	0.017438

3 33		
-0.023512	-0.001904	-0.030247
-0.007346	-0.010305	0.006701
0.011677	0.004144	-0.002725
-0.001412	0.005158	0.006367
0.003024	0.022217	-0.011963
-0.008178	-0.017476	0.019363
-0.012227	-0.001455	-0.023205
0.004326	0.005620	0.009935
0.011496	0.006435	-0.021082
-0.006169	-0.009929	0.003945
-0.026289	0.000369	-0.025867
0.002598	-0.005185	0.058432
-0.004254	-0.013330	0.000837
0.001884	0.000901	-0.004328
-0.011071	0.002873	0.005348
-0.008974	0.004680	-0.000260
-0.013585	0.011910	0.033620

APPENDIX Continued

0.003810	-0.006552	0.023357
0.000226	0.002504	0.074808
-0.016259	-0.001787	0.020052
-0.039548	0.005946	0.001078
-0.059274	-0.001609	-0.029806
0.423062	-0.680696	0.312992
0.403246	-0.441504	-0.550044
-1.208292	-3.378815	-0.558792
-3.854346	0.689827	-0.915930
4.951425	-0.506458	3.281277
1.062392	1.702347	0.052524
0.375232	0.419508	0.086708
0.210874	-1.456524	0.288606
-0.556610	-0.071725	0.565068
0.099234	-0.080449	0.767901
0.411513	-0.675125	0.893456

1 36		
-0.013269	-0.187572	-0.160551
0.036391	-0.027755	-0.032635
-0.036675	0.021763	-0.001006
0.001900	0.034456	0.185204
0.050760	-0.014107	-0.171911
-0.133974	0.003369	0.122298
-0.003684	0.008030	-0.154843
0.016575	0.030146	0.055324
-0.011092	0.015818	-0.024466
0.010554	0.115628	0.045005
0.079245	-0.035660	-0.415293
0.203598	1.147286	0.040564

1 30		
-0.170635	-0.001781	0.041474
-0.033369	0.020098	0.011473
0.023607	-0.019211	-0.017678
-0.004035	-0.008876	-0.005405
0.000469	-0.002737	0.008525
0.003027	0.031736	0.036755
-0.013343	0.003321	-0.004641
0.002457	-0.028200	-0.009667

0.009025	0.013701	0.018687
0.045799	0.010368	-0.006010